IMU-based image stabilization in a HSM-driven camera positioning unit

Riccardo Antonello
Roberto Oboe
Davide Pilastro
Simone Viola
Department of Management Eng.
University of Padova
Vicenza, Italy, 36100
Email: riccardo.antonello@unipd.it
roberto.oboe@unipd.it

Kazuaki Ito
Dept. of Electrical and Electronic Eng.
Toyota National College of Technology
Toyota, 4718525, Japan
E-mail: kazu-it@toyota-ct.ac.jp

Angelo Cenedese
Department of Information Eng.
University of Padova
Padova, Italy, 35131
E-mail: angelo.cendese@unipd.it

***Abstract*—Camera positioning units are widely used in surveillance and they are sometimes mounted on floating supports, e.g. on patrolling ships or buoys. The support motion, in turn, induces an apparent motion in the image plane, which can create troubles to the image processing, especially when a specific feature must be tracked (e.g. a distant ship, getting close to a forbidden area). Low cost devices are often characterized by low frame rate and low image resolution, for which traditional image stabilization techniques usually results to be rather ineffective. Additionally, low-end camera units are usually driven by hybrid stepper motors and, being conceived to work in an harsh environment, they do not mount any optical image stabilization (OIS) system, either in the camera lenses or in the image sensor. In this paper, the image acquired by a pan–tilt camera positing unit mounted on a moving support is stabilized by exploiting the camera attitude information provided by a MEMS-based IMU with an embedded magnetometer. In particular, two independent integral control loops are designed for the pan and tilt motors in order to compensate for the yaw and pitch motions of the support. As for the roll motion, since it relates to an unavailable degree of freedom in the positioning unit, it can be compensated only on the captured image. The proposed solution is experimentally tested on a real device mounted on a moving table actuated by a 6 degrees–of–freedom pneumatic hexapod. Realistic motions are recreated by using the data recordings taken aboard of a patrolling ship and a costal buoy. Experimental results show that the proposed solution is capable of keeping the camera pointing at a fixed target with a good accuracy, thus making higher-level image processing easier and more effective.**

I. Introduction

Camera positioning units, such as *pan–tilt–zoom* (PTZ) units, are often used in surveillance applications to reorient the camera *line of sight* (LOS) in order to fulfill some specific task, such as patrolling a wide area or tracking a specific moving target [1]. In many circumstances, these units are installed on non-inertial supports, such as on top of long poles (which bend in case of wind gusts), or on board of ground vehicles, ships, floating buoys, aircrafts, etc. In this situations, the support motion causes an apparent motion of the camera *field of view* (FOV) that could make the surveillance task problematic. In order to obtain clear and steady images, despite the support motion, an *optical image stabilization* (OIS) system must be exploited. Several OIS techniques can be directly implemented on the camera device, either as hardware or software compensations: in the former case, the camera lenses or the image sensor (CCD detector) are moved or deformed in order to compensate for the support motion measured by some inertial sensor mounted on the camera frame, while in the latter case some real-time image processing algorithms (e.g. *deblurring* algorithms) perform a frame–to–frame image correlation to estimate and remove the motion of the camera FOV. Unfortunately, both the aforementioned solutions are unsuitable for low cost devices, in which the installed cameras have a low frame rate and are required to operate in harsh conditions. A viable alternative to the previous camera built-in OIS systems consists of using the camera positioning unit to implement an *inertially stabilized platform* (ISP), which is a mechanism capable of holding the orientation of its payload (e.g. the camera device) steady with respect to an inertial frame [2]. When used for OIS applications, the ISP is requested to hold the camera LOS steady in inertial space, along the selected orientation. This task is usually accomplished by installing the camera on a motorized gimbal assembly, which allows to control the rotations about two independent axes orthogonal to the LOS. The information required to stabilize the LOS is usually provided either by a set of gyroscopes, which measure rotations (angular rates) in inertial space [3], or even by a complete *inertial measurement unit* (IMU), which directly provides an estimate of its attitude with respect to an inertial frame [4]. It is worth noticing that the LOS stabilization performed with the aid of a two–axis gimbal support implies only the stabilization of the center of the camera FOV: in fact, any rotation of the camera along the LOS cannot be removed by a two–axis gimbal. To stabilize the orientation of the camera FOV, either an additional controlled axis must be introduced (by using a multi–axis gimbal), or the image must be rotated (via image–processing) by the (opposite) angular displacement undergone by the camera along the LOS.

In this paper, the ISP–based approach described above is

978-1-4673-1388-9/13/$31.00 ©2013 IEEE

applied to stabilize the FOV of a camera mounted on a low cost pan–tilt positioning unit, driven by a pair of hybrid stepper motors (HSMs). The inertial measurements required for the image stabilization are retrieved by employing a low cost MEMS–based IMU with an embedded magnetometer, which is directly attached to the camera frame. The unit is mounted in such a way that its axes, namely the yaw, pitch and roll axes, are aligned with, respectively, the pan, tilt and zoom axes of the camera positioning unit. The center of the camera FOV (i.e. the camera LOS) is stabilized by controlling the pan and tilt motors with two independent integral control loops that use the yaw and pitch angle measurements provided by the IMU; instead, the orientation of the camera FOV is stabilized by rotating the image acquired by the camera by the roll angle measurement provided by the sensor.

The paper is organized as follows. Sec. II contains a description of the camera positioning unit used to test the proposed IMU–based image stabilization system. In Sec. III it is explained how the camera frame attitude is estimated in the inertial space by using the measurements provided by a MEMS–based IMU with an embedded magnetometer. The design of the two integral regulators controlling the pan and tilt HSMs is presented in Sec. IV. All the information pertaining the experimental tests performed in laboratory are reported in Sec. V. Finally, some considerations and conclusions are provided in Sec. VI.

II. Camera positioning unit

This paper deals with low cost camera positioning units for surveillance applications, such as the one shown in Fig. 1. The unit is designed to operate outdoor, where it has often to face harsh environmental conditions in terms of temperature and humidity levels. It can be installed on different types of steady or moving supports, ranging from concrete walls or long poles to floating buoys and patrolling ships.

The unit allows to rotate the camera along its pan and tilt axes, which are respectively perpendicular and parallel to the unit base. The motion along the two axes is generated by a pair of hybrid stepper motors (HSMs), which are connected to the load by means of a reduction unit composed of two gears and a toothed belt. The advantage of using HSMs mainly relies in their capability of performing an accurate positioning without requiring any position sensor either at the motor or the load side, thus reducing the overall cost of the motion control system. In order to reduce the torque ripple that could be amplified by the elastic transmission system, yielding a non–smooth motion with large residual vibrations, the two HSM motors are driven in micro–stepping mode [5].

III. Camera orientation estimation

A. MEMS–based Inertial Measurement Unit

A compact, low cost MEMS–based Inertial Measurement Unit (IMU) is used to provide the information required for the stabilization of the camera FOV. Such choice is motivated by the reduced cost of the device, and the fact that its limited size and weight allow an easy installation on

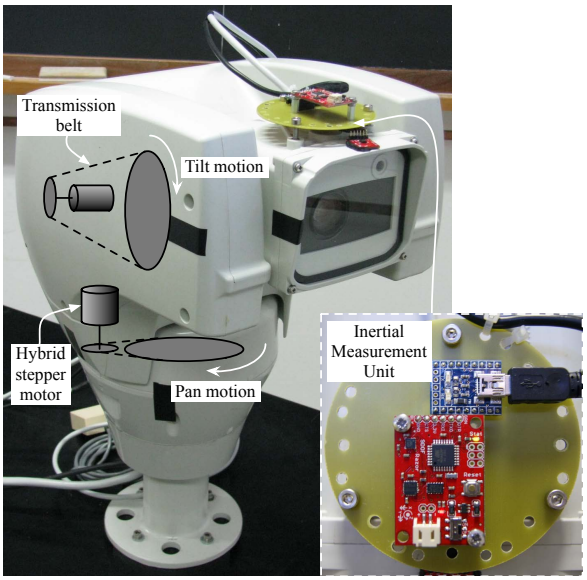

(a)

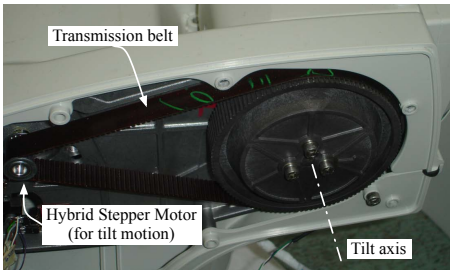

(b)

Fig. 1. Camera positioning unit details: (a) location of the pan and tilt motion systems, composed both by a transmission toothed–belt driven by a hybrid stepper motor. On top of the camera frame is visible the MEMS–based inertial measurement unit used to estimate the camera attitude in the inertial space; (b) expanded view of the tilt motion system.

existing systems. A single unit generally embeds a three–axis accelerometer/gyroscope pair; additionally, a three–axis magnetometer is usually included in the unit to provide the heading information with respect to the Earth's magnetic axis. With the aid of a sensor fusion algorithm, the sensor data can be combined together to extract the estimate of the IMU attitude in inertial space, thus transforming the IMU in a fully functional *attitude and heading reference system* (AHRS).

Regarding the installation of the IMU on the camera positioning unit, two options are available, namely either at the unit base or on its payload (i.e. camera frame). Among the two options, the latter is chosen, because it allows to get a direct measurement of the payload (angular) position, which would be otherwise unknown since no other position sensors are installed on the unit.

B. Sensor fusion algorithm

An off–the–shelf sensor fusion algorithm [6] has been adopted for processing the measurements provided by the IMU, in order to extract an estimate of the camera orientation,

in terms of roll, pitch and yaw angles in inertial space.

The algorithm operates as a nonlinear observer on the special orthogonal group $SO(3)$ (i.e. the attitude is represented in terms of *direct cosine matrices* – DCMs), driven by the attitude reconstructed from the accelerometers, the angular velocity measured by the gyroscopes and the heading information provided by the magnetometer. Overall, it can be described as follows:

1) the algorithm estimates the current value of the DCM matrix $\boldsymbol{C}_b^i$, which represents the attitude of the body (e.g. IMU) frame in the inertial frame coordinates, by performing a one-step numerical integration over time of the well known kinematic equation describing the time derivative of a rotation matrix [7]
$$\frac{d\boldsymbol{C}_b^i}{dt} = \boldsymbol{C}_b^i \, (\boldsymbol{\omega}_{i/b}^b)_\times \, , \quad (\boldsymbol{\omega}_{i/b}^b)_\times \triangleq \begin{bmatrix} 0 & -\omega_z & \omega_y \\ \omega_z & 0 & -\omega_x \\ -\omega_y & \omega_x & 0 \end{bmatrix} \tag{1}$$
that expresses how the body attitude changes over time when the body frame rotates with respect to the inertial frame at a rate $\boldsymbol{\omega}_{i/b}^b = [\omega_x, \omega_y, \omega_z]^T$, as specified in body frame coordinates. A direct measurement of the vector $\boldsymbol{\omega}_{i/b}^b$ is provided by the three-axis gyroscope mounted on–board of the IMU.
2) the numerical integration of (1) introduces small errors that may accumulate over time, thus yielding an estimate of the matrix $\boldsymbol{C}_b^i$ which is not an orthonormal matrix (i.e. an element of $SO(3)$). Therefore, in order to avoid this issue, at the end of each integration step an orthonormalization procedure is applied to the columns of the current estimate of the DCM matrix $\boldsymbol{C}_b^i$.
3) the angular rate measurement provided by a MEMS gyroscopes is usually affected by non–negligible bias and (slowly varying) drift errors that may accumulate over time when integrating (1), thus yielding a wrong estimate of the body attitude. In order to compensate for the effect of the gyroscope bias and drift, the misalignments between the estimated and measured magnetic field and gravity vectors in body frame coordinates are used to compute a compensation term for the angular rate measurement used in the integration of (1). The compensation term is actually computed as the output of a PI regulator that forces the misalignment errors to converge to zero, at a faster rate than their natural rate of growth.

A more detailed description of the sensor fusion algorithm can be found in [8].

IV. Inertial stabilization of the camera FOV

As already pointed out in the introduction, the center of the camera FOV (i.e. its LOS) is stabilized by controlling the pan and tilt motors with two independent control loops, whose aim is to regulate the estimated yaw and pitch angles of the camera frame (as retrieved by processing the IMU data with the algorithm described in Sec. III-B) to some specific set–points. The design of the two control loops must take into account the fact that the stepper motors used for the pan and tilt motions are position–driven actuators, and the position reference has to change at a limited rate, in order to prevent step–losses phenomena. A simple way to enforce such limitation consists of using an integrator with saturated input to generate the motor position command, as shown in Fig. 2

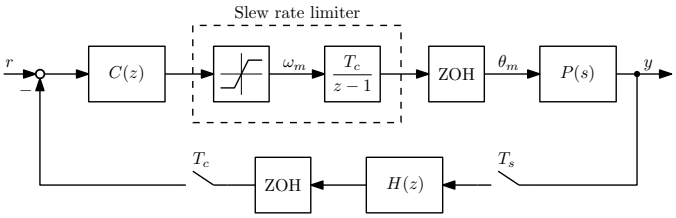

Fig. 2. Simplified block diagram of the HSM servo–loop used to inertially stabilize both the pan and tilt axes of the camera positioning unit. In the block diagram, $P(s)$ represents the pan/tilt dynamics from the motor position command θ_m to the unit pan/tilt angle y, while $H(z)$ denotes the sensor (i.e IMU/AHRS) dynamics. The motor controller $C(z)$ and the inertial sensor $H(z)$ operate at two different rates, with the former being usually faster than the latter.

Then, the pan/tilt regulation loops can be designed with conventional methods, after remarking that the actual plant to be controlled now includes an additional integrator in its transfer function. With reference to the identified frequency responses of the pan and tilt motion systems reported in Fig. 3, measured from the motor input, i.e. the rotor position command, to the pan and tilt angles of the camera positing unit, it can be deduced that either a proportional or a proportional–integral (PI) regulator is sufficient to stabilize the closed loop system with a satisfactory phase margin (almost $90°$ for small gain crossover frequencies). In practice, the pan and tilt controllers have been designed (using Bode's method) as two conventional

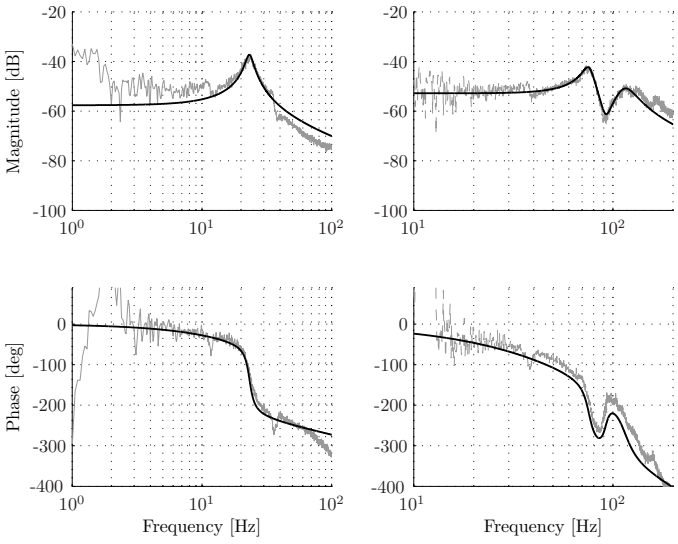

Fig. 3. Nonparametric (gray thin line) and parametric (black thick line) identification of the pan (left column plots) and tilt (right column plots) dynamics, under the assumption of no motor step–losses. The two frequency responses shown in figure are evaluated from the pan/tilt motor position command to the unit pan/tilt angular displacement.

PI controllers capable of achieving a $\varphi_m = 50°$ phase margin at the gain crossover frequencies of, respectively, $\omega_{gc} = 0.5\,\text{Hz}$ for the pan motion and $\omega_{gc} = 1.0\,\text{Hz}$ for the tilt motion. The design results are reported in Fig. 4.

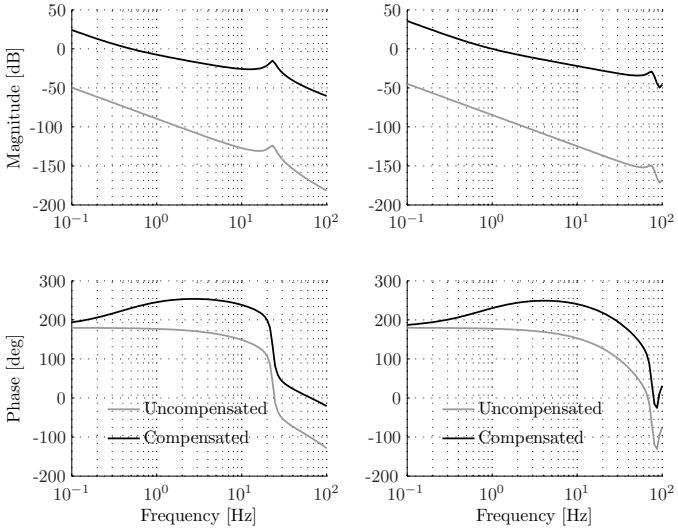

PI controller gains

Gain	Symbol	Pan dynamics	Tilt dynamics
Proportional	K_P	$\approx 1.9 \cdot 10^6$	$\approx 2.2 \cdot 10^6$
Integral	K_I	$\approx 4.7 \cdot 10^6$	$\approx 10.5 \cdot 10^6$

Fig. 4. Open loop frequency responses of the uncompensated (gray line) and compensated (black line) pan (left column plots) and tilt (right column plots) dynamics.

V. Experimental results

A. Experimental setup

The proposed image stabilization system described in the previous section has been tested in laboratory with the aid of the experimental setup shown in Fig. 5. In practice, the camera positioning unit has been mounted on top of a 6 degrees of freedom (DOF) pneumatic hexapod (*Stewart platform*) in order to impress a controlled motion to the unit base. An independent joint controller has been implemented to control the pose (i.e. position and orientation) of the movable platform of the hexapod in inertial space.

The IMU used to estimate the camera frame orientation in inertial space is a *Sparkfun's 9DOF Razor IMU*, which is a low cost commercial MEMS–based IMU equipped with a three–axis accelerometer/gyroscope/magnetometer triad and a micro-controller (*ATMega328*) that can be used to perform the sensor fusion directly aboard of the IMU device. In particular, a firmware implementing the sensor fusion algorithm described in Sec. III-B is available at no charge on the manufacturer website [9].

B. Experimental tests

In order to test the effectiveness of the proposed image–stabilized camera positing unit under rather realistic operating

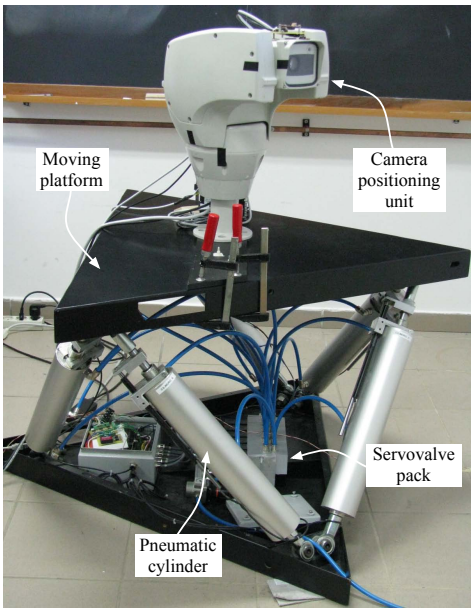

Fig. 5. 6–DOF pneumatic hexapod used during the experimental tests.

conditions, the motion data recorded aboard of two different floating supports, namely a coast guard patrolling ship and a costal buoy, has been used to generate the hexapod movements. The data recordings has been extracted from [10]. Two tests have been carried out to obtain a quantitative assessment of the image stabilization:

1) the camera attitude measurements obtained on an image–stabilized camera unit have been compared to those recorded on an uncompensated camera operating under the same conditions, i.e. with the same support motion.
2) the jitter of the camera FOV center on the image plane has been evaluated by pointing the camera on a structured scenario, from which a fixed target (in inertial space) can be easily identified and tracked. A simple scenario consisting of a cross with two black orthogonal arms, drawn on a white background, has been used for the laboratory experiments. Such choice has been motivated by the fact that all the relevant information about the orientation of the camera FOV and the location of its center can be determined by simply measuring the position and orientation of the cross on the image plane. This operation implies the detection of the two cross arms on the image plane, which can be done by applying a Hough transform [11] at each frame acquired with the camera. Then, the fluctuations of the cross center on the image plane, induced by the support motion, can be used to evaluate the stability of the camera FOV center.

Indeed, these two tests are designed to evaluate the stability level of the camera LOS; as for the camera FOV orientation, all the tests performed in laboratory consisted in a visual inspection of the acquired video stream, so that no quantitative results can be reported in this paper.

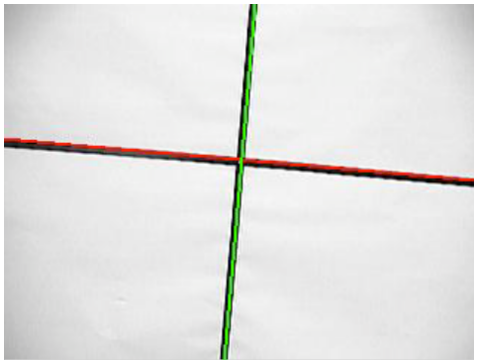

Fig. 6. Typical frame of the post-processed camera video output. The output of the line detection procedure based on the Hough transform (red and green lines) is superimposed on the original video frame (cross with two black arms on a white background) for convenience reasons. In the acquired frame, the axes of the camera FOV appear to be misaligned with those of the fixed reference target (e.g. black cross) in inertial space.

C. Experimental results

The results of the experimental tests performed by using the motion data recorded aboard of a coast guard patrolling ship are collectively reported in Figs. 7 and 9.

From Fig. 7 it can be noticed that the inertial stabilization of the camera frame is more effective on the yaw axis, rather than the pitch axis. This is probably due to the fact that the HSM servo–loop of the pan motion is less reactive to the (yaw angle) measurement noise than the servo–loop for the tilt motion, since it has to drive a larger inertia. As expected, note that the the roll angle measurement is unaffected by the inertial–stabilization system.

The capability of the proposed image–stabilization system to keep the camera pointing at a fixed target can be judged also by visualizing the wandering motion, on the image plane, of the camera FOV center, as analyzed in Fig. 9.

Similar results to those reported in Figs. 7 and 9 are shown in Figs. 8 and 10, with the only difference that now the experiments are performed by using the motion data recorded aboard of a coastal buoy, instead of a patrolling ship.

VI. Conclusions

The compensation of the support motion in a camera positioning unit is can be performed in several ways, by acting on the optical equipment (lenses or image sensor) or on the acquired image stream. In this paper we propose a different approach that can be applied as a retrofit on existing system, by exploiting inertial measurements provided by a set of MEMS sensors and magnetometers. It is worth noticing that such sensors can be already found in advanced camera positioning units, where they are used for active vibration damping and ripple torque minimization (see e.g. [12]). The proposed approach has demonstrated experimentally to largely improve the image tracking capabilities, under realistic conditions. Some limitations have been found, due to the use of

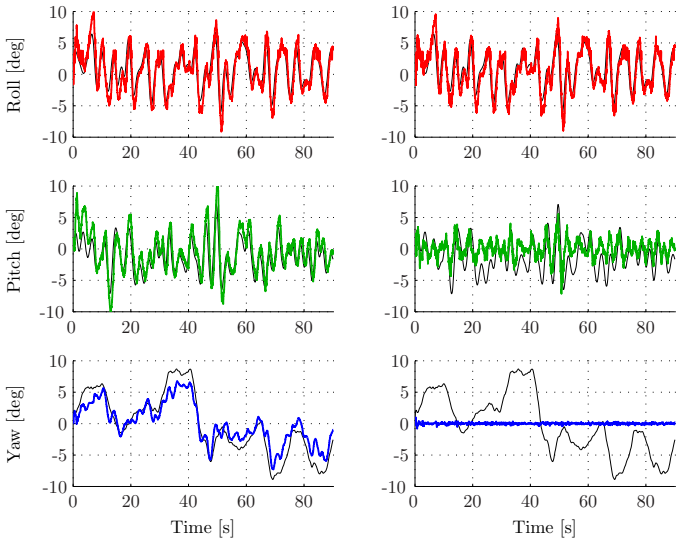

Standard deviations

Angle	Symbol	Before comp. [deg]	After comp. [deg]
Roll	σ_R	4.02	3.83
Pitch	σ_P	3.46	1.33
Yaw	σ_Y	3.12	0.13

Fig. 7. Roll, pitch and yaw angles of the camera frame, as measured on an uncompensated (left column plots) and an inertially stabilized (right column plots) positioning unit. The reference data used to generate the motion are shown with thin black lines.

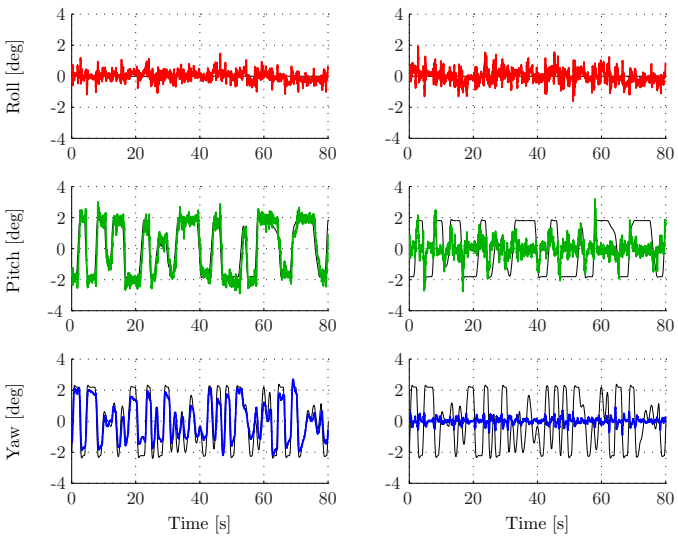

Standard deviations

Angle	Symbol	Before comp. [deg]	After comp. [deg]
Roll	σ_R	0.31	0.38
Pitch	σ_P	1.71	0.61
Yaw	σ_Y	1.22	0.20

Fig. 8. Same as Fig. 7, but for the case of a motion generated by using the data recordings taken aboard of a coastal buoy, instead of a patrolling ship. Note that no roll angle recordings were available in this dataset, and hence the roll angle reference motion (thin black line) is constantly equal to zero.

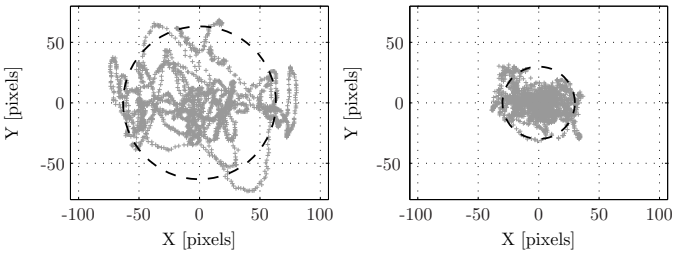

Standard deviations

Direction	Symbol	Before comp. [pixels]	After comp. [pixels]
x–axis	σ_x	38.79	16.94
y–axis	σ_y	23.65	10.45
radial	σ_r	21.09	9.98

Fig. 9. Jittering motion on the image plane of the camera FOV center, as measured on an uncompensated (left plot) and an inertially stabilized (right plot) positioning unit. On each plot, the dashed circle represents the $3\,\sigma_r$ boundary of the distribution of the camera FOV centers.

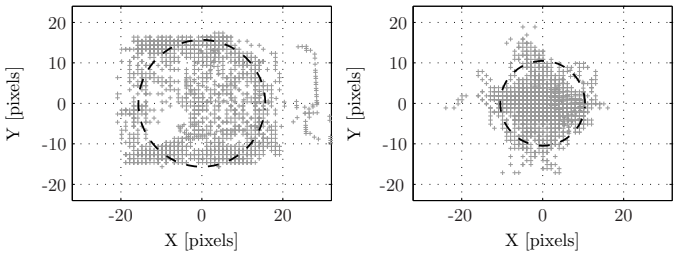

Standard deviations

Direction	Symbol	Before comp. [pixels]	After comp. [pixels]
x–axis	σ_x	12.06	5.31
y–axis	σ_y	11.28	4.21
radial	σ_r	5.22	3.50

Fig. 10. Same as Fig. 9, but for the case of a motion generated by using the data recordings taken aboard of a coastal buoy, instead of a patrolling ship.

off-the-shelf algorithms for the computation of the camera orientation. Better results, especially in terms of measurement noise and consequent camera residual vibrations, are expected by using more advanced filtering techniques. This will be a subject of a future research.

ACKNOWLEDGMENTS

The authors would like to thank Roberto Losco for his support in the preparation of the experimental system, and Videotec S.p.a. (Schio - Italy) for providing the camera positioning unit used in the laboratory tests.

REFERENCES

[1] J. Nygårds, P. Skoglar, M. Ulvklo, and T. Högström, "Navigation aided image processing in uav surveillance: Preliminary results and design of an airborne experimental system," *Journal of Robotic Systems*, vol. 21, no. 2, pp. 63–72, 2004. [Online]. Available: http://dx.doi.org/10.1002/rob.10128

[2] J. Hilkert, "Inertially stabilized platform technology: Concepts and principles," *Control Systems, IEEE*, vol. 28, no. 1, pp. 26 –46, feb. 2008.

[3] Z. Hurak and M. Rezac, "Image-Based Pointing and Tracking for Inertially Stabilized Airborne Camera Platform," *Control Systems Technology, IEEE Transactions on*, vol. 20, no. 5, pp. 1146 –1159, sept. 2012.

[4] M. Masten, "Inertially stabilized platforms for optical imaging systems," *Control Systems, IEEE*, vol. 28, no. 1, pp. 47 –64, feb. 2008.

[5] T. Kenjo, *Stepping Motors and Their Microprocessor Controls*. Oxford: Clarendon Press, 1984.

[6] Tutorial: Building an AHRS/Head-tracker using the 9DOF Razor IMU. [Online]. Available: https://dev.qu.tu-berlin.de/projects/sf-razor-9dof-ahrs/wiki/Tutorial

[7] M. W. Spong, S. Hutchinson, and M. Vidyasagar, *Robot Modeling and Control*. Wiley, 2005.

[8] R. Mahony, T. Hamel, and J.-M. Pflimlin, "Nonlinear Complementary Filters on the Special Orthogonal Group," *Automatic Control, IEEE Transactions on*, vol. 53, no. 5, pp. 1203 –1218, june 2008.

[9] Sparkfun's 9–DOF Razor IMU webpage. [Online]. Available: https://www.sparkfun.com/products/10736

[10] Thompson, J. L and R.A.N. Research Laboratory, "Ship motion measurements made on an Attack Class patrol boat (HMAS Bombard)," Report, 1980.

[11] D. Forsyth and J. Ponce, *Computer vision: a modern approach*. Prentice Hall, 2002.

[12] R. Antonello, A. Cenedese, and R. Oboe, "Use of MEMS gyroscopes in active vibration damping for HSM-driven positioning systems," in *IECON 2011 - 37th Annual Conference on IEEE Industrial Electronics Society*, nov. 2011, pp. 2176 –2181.